Journal of Medicinal Chemistry

Article

pubs.acs.org/jmc

Going Out on a Limb: Delineating The Effects of β-Branching, *N*-Methylation, and Side Chain Size on the Passive Permeability, Solubility, and Flexibility of Sanguinamide A Analogues

Andrew T. Bockus,[†] Joshua A. Schwochert,[†] Cameron R. Pye,[†] Chad E. Townsend,[†] Vong Sok,[†] Maria A. Bednarek,[‡] and R. Scott Lokey*[,†]

[†]Department of Chemistry and Biochemistry, University of California, Santa Cruz, California 95064, United States

[‡]Department of Antibody Discovery & Protein Engineering, Medimmune Ltd, Cambridge CB21 6GH, United Kingdom

Supporting Information

ABSTRACT: It is well established that intramolecular hydrogen bonding and *N*-methylation play important roles in the passive permeability of cyclic peptides, but other structural features have been explored less intensively. Recent studies on the oral bioavailability of the cyclic heptapeptide sanguinamide A have raised the question of whether steric occlusion of polar groups via β-branching is an effective, yet untapped, tool in cyclic peptide permeability optimization. We report the structures of 17 sanguinamide A analogues designed to test the relative contributions of β-branching, *N*-methylation, and side chain size to passive membrane permeability and aqueous solubility. We demonstrate that β-branching has little effect on permeability compared to the effects of aliphatic carbon count and *N*-methylation of exposed NH groups. We highlight a new *N*-methylated analogue of sanguinamide A with a Leu substitution at position 2 that exhibits solvent-dependent flexibility and improved permeability over that of the natural product.

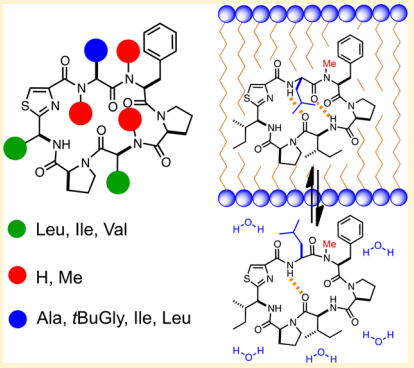

INTRODUCTION

Recent efforts to understand the absorption, distribution, metabolism, and excretion (ADME) properties of cyclic peptides have been driven by a growing interest in their potential in the development of next-generation therapeutics.[1−4] Studies on cyclic peptide scaffolds have yielded insights into the importance of conformation,[5−22] *N*-methylation,[6,11,23−27] occlusion of polar groups from solvent,[6−8,16,28−31] molecular size,[32−34] solubility,[11,26] and lipophilicity,[5,33,35] in determining ADME properties.[34,36,37] Though strides have been made using model systems containing proteinogenic and uncommon amino acids,[6−10,12,16,17,23,30,31,37−40] a comprehensive understanding of the structural determinants that drive passive permeability in cyclic peptide natural products remains elusive.

Though *N*-methylation of exposed NH groups is considered an effective method for enhancing passive permeability in cyclic peptides, nature may use other strategies as well. For example, β-branched amino acids such as Ile and Val are enriched in cyclic peptide natural products and could serve to sterically occlude solvent-exposed NH groups or impart conformational rigidity by limiting rotation of the ϕ and ψ angles.[41] Alternatively, nature may optimize permeability by balancing exposed polar surface area with lipophilic side chains.

Sanguinamide A, a thiazole-containing cyclic heptapeptide with two β-branched side chains, demonstrates low cell permeability and modest oral bioavailability (~7%) in rat (Figure 1).[30,31,42] Though the structure contains two transannular hydrogen (H−) bonds, the solvent-exposure of a third

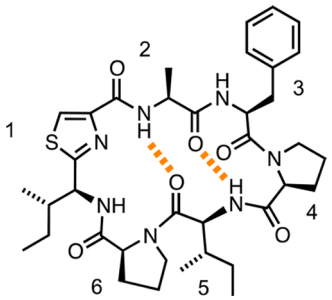

Figure 1. Sanguinamide A (**1**). An orally bioavailable cyclic heptapeptide from the nudibranch *Hexabranchus sanguineus* with the two transannular hydrogen bonds as previously elucidated by temperature shift coefficients, H/D-exchange studies, and the NMR solution structure in DMSO.[31,42]

phenylalanine NH may explain the suboptimal physicochemical properties of the cyclic peptide.[31] Nielsen et al. previously employed Ala-to-*tert*-butylglycine (*t*BuGly) substitution and Phe3 *N*-methylation on this scaffold to generate the danamides, one of which had oral bioavailability of 51% in rat.[30] Their results suggested that solvent exposure of the amide NH could be offset by the large *tert*-Bu side chain and its ability to shield the polar core of the molecule, although the specific impact of β-branching was not parsed from the effect of simply increasing the aliphatic

Received: June 15, 2015
Published: August 26, 2015

Downloaded via UNIV TOWN OF SHENZHEN on February 27, 2021 at 06:50:05 (UTC).
See https://pubs.acs.org/sharingguidelines for options on how to legitimately share published articles.

© 2015 American Chemical Society

DOI: 10.1021/acs.jmedchem.5b00919
J. Med. Chem. 2015, 58, 7409−7418

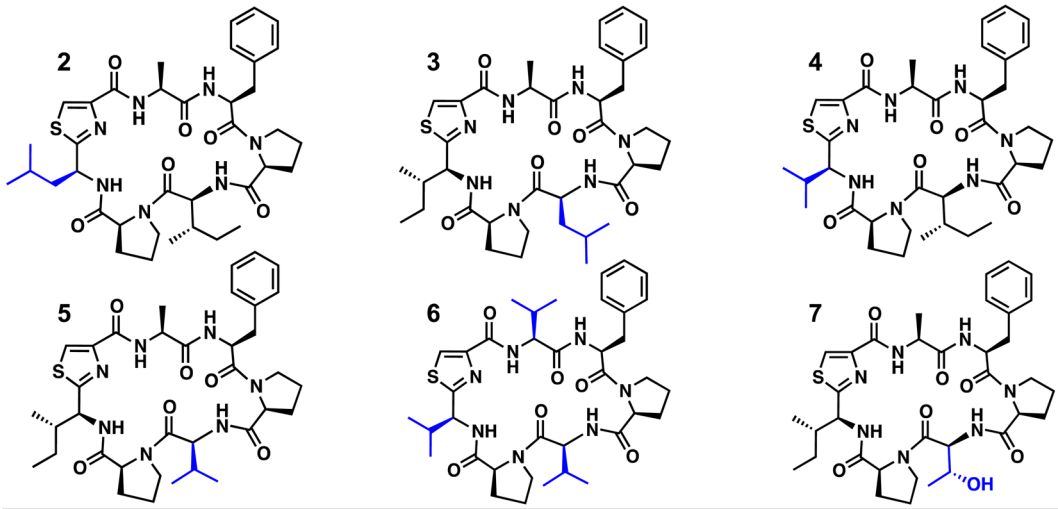

cpd	AlogP	PAMPA P_e (x 10^{-6} cm s^{-1})	Caco-2 P_{app} (x 10^{-6} cm s^{-1})	50% Isocratic RT (min)	Solubility Limit in PBS (μM)	
					Kinetic	Thermodynamic
1	2.86	5.3 ± 2.2	1.3 ± 0.2	2.77	147-159	107 ± 20
2	2.80	5.6 ± 2.0	1.3 ± 0.3	2.87	182-222	35 ± 61
3	2.80	5.3 ± 1.3	0.2 ± 0.2	2.19	133-153	122 ± 78
4	2.41	4.8 ± 0.7	3.7 ± 0.5	2.03	285-315	205 ± 89
5	2.41	4.9 ± 1.5	0.3 ± 0.3	1.97	182-222	236 ± 17
6	2.79	4.7 ± 0.3	2.2 ± 0.1	2.81	105-118	148 ± 4
7	1.05	0.2 ± 0.0	0.4 ± 0.1	1.02	285-400	-

Figure 2. *β*-Branched analogues of sanguinamide A. **2** Ile1Leu, **3** Ile5Leu, **4** Ile1Val, **5** Ile5Val, **6** Ile1Val/Ala2Val/Ile5Val, **7** Ile5Thr. Compounds **2**, **3**, and **6** have the same aliphatic carbon count as the parent scaffold (**1**) while **4**, **5**, and **7**, have fewer. Compounds **3** and **5** were measured near the detection limit of the Caco-2 assay.

carbon count in the Ala to *t*BuGly substitution. The multitude of modifiable features in sanguinamide A (*β*-branched aliphatic side chains, and free amides) make it an excellent subject for more systematic structure−property relationship studies designed to further elucidate the influence of discrete modifications that may impact passive permeability and other important physical properties. Therefore, we set out to investigate the passive permeabilities, solubilities, relative lipophilicities, and amide temperature coefficients (T_c-NH) of analogues of sanguinamide A that vary in backbone *N*-methylation, as well as in the size, location, and degree of branching in the side chains. Our results show that *β*-branching imparts a minimal effect, if any, on the permeability of the sanguinamide scaffold. Rather, improvements to passive permeability are primarily driven by a combination of *N*-methylation and an increase in scaffold lipophilicity resulting from the introduction of larger aliphatic side chains. *N*-methylated analogues containing natural amino acids with less *β*-branching than *t*BuGly (Leu and Ile) were just as cell-permeable as the danamides. These data suggest that, to improve the permeability of an already semipermeable scaffold, removal of H-bond donors (*N*-methylation or H-bond formation) is preferable to steric occlusion, and increased lipophilicity can compensate for a lack of *N*-methylation. We also report an *N*-methylated scaffold, **17**, that is highly permeable in both PAMPA and Caco-2 assays and has noteworthy solubility, which we attribute to solvent-dependent conformational flexibility.

RESULTS

To investigate the effects of *β*-branching, *N*-methylation, and side chain size on passive permeability and other physicochemical properties, we synthesized 17 sanguinamide A analogues including the parent scaffold and two of the previously reported danamides (F, **12** and D, **15**).[30]

***β*-Branching.** Analysis of the AntiMarin and ProtScale[43] databases revealed a significantly larger Ile:Leu ratio in uncharged cyclic peptides compared to that found in proteins (Table S1). The Ile:Leu ratio was even more pronounced among compounds in the ribosomally derived patellamide family of cyclic peptides,[44] whose members are passively permeable[22] and share some structural similarity with sanguinamide A (Figure 1). Furthermore, Nielsen et al., discovered that substitution of the Ala3 in sanguinamide A with a highly branched *t*BuGly led to an improvement in the compound's ADME properties,[30] consistent with observations from our group that steric occlusion of polar groups can outweigh internal hydrogen bonding in determining the passive membrane permeability of cyclic peptide scaffolds.[16] Together these observations bolster the hypothesis that *β*-branching may provide an alternative or complementary mechanism for enhancing passive membrane permeability in cyclic peptide natural products.

In the NMR solution structure of sanguinamide A (Figure 1) in DMSO,[31] both Ile1 and Ile5 hydrophobically shield the polar core of the molecule. We hypothesized that Ile-to-Leu substitutions would reduce steric occlusion of polar groups near these side chains and decrease permeability (Figure 2).

DOI: 10.1021/acs.jmedchem.5b00919
J. Med. Chem. 2015, 58, 7409−7418

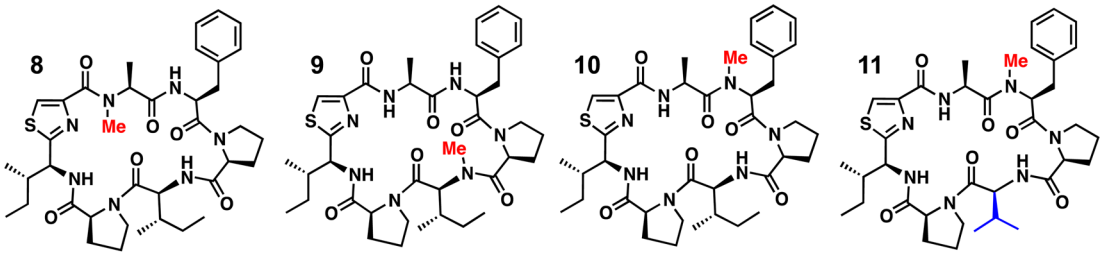

cpd	AlogP	PAMPA P_e (x 10^{-6} cm s^{-1})	Caco-2 P_{app} (x 10^{-6} cm s^{-1})	50% Isocratic RT (min)	Solubility Limit in PBS (μM)	
					Kinetic	Thermodynamic
8	3.07	0.5 ± 0.1	0.2 ± 0.0	1.48	333-500	801 ± 13
9	3.07	1.3 ± 0.1	0.4 ± 0.1	1.79	-	-
10	3.07	11.0 ± 1.1	7.4 ± 0.4	3.03	105-118	172 ± 9
11	2.61	9.1 ± 1.2	6.8 ± 0.7	2.24	133-153	296 ± 5

Figure 3. Methylated analogues of sanguinamide A. **8** Ala2(NH) → (NMe), **9** Ile(NH) → (NMe), **10** Phe(NH) → (NMe), **11** Phe(NH) → (NMe)/Ile5Val. Compounds **8**, **9**, and **10** have an addition methyl, while compound **11** has the same number of aliphatic carbons as the parent.

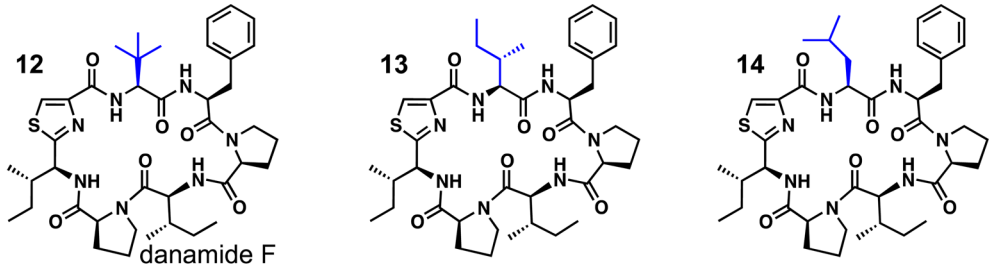

cpd	AlogP	PAMPA P_e (x 10^{-6} cm s^{-1})	Caco-2 P_{app} (x 10^{-6} cm s^{-1})	50% Isocratic RT (min)	Solubility Limit in PBS (μM)	
					Kinetic	Thermodynamic
12	4.19	2.2 ± 0.3	8.0 ± 2.0	8.72	36-44	8 ± 2
13	4.37	6.1 ± 0.5	9.6 ± 0.2	7.86	39-41	6 ± 9
14	4.30	4.7 ± 2.2	10.9 ± 1.2	9.13	39-41	10 ± 5

Figure 4. Butyl (blue) analogues of sanguinamide A. **12** Ala2*t*BuGly, **13** Ala2Ile, **14** Ala2Leu. Danamide F, **12**, was previously reported to have impressive cell permeability and oral bioavailability.[30]

Since Val is also branched at the beta position, we hypothesized that Ile-to-Val substitutions would maintain permeability despite an overall decrease in the lipophilicity of the side chain.

These *β*-branched substitutions had little effect on permeability as measured by PAMPA and the Caco-2 live cell assay. All compounds fell on the low end of the permeability spectrum. The addition of a backbone −OH in **7** diminished permeability even further. Although minor differences in Caco-2 permeability, HPLC retention time, and solubility were observed across the series, these effects were small in magnitude and, taken together, suggest that overall, *β*-branching has a negligible on permeability in this series.

***N*-Methylation.** An ever-growing body of research suggests that *N*-methylation can enhance the permeability of cyclic peptide scaffolds by removing hydrogen bond donors and, in some cases, stabilizing lipophilic conformations.[6,11,24,26] This effect has also been demonstrated with sanguinamide A analogues, although the effect of *N*-methylation on the parent compound itself was not reported.[30] To further investigate the effect of backbone *N*-methylation on the permeability of the sanguinamide A scaffold, we synthesized a series of four *N*-methyl analogues (Figure 3). As expected, the effect of *N*-methylation on permeability was highly position-dependent. Only *N*-methylation of the exposed Phe3-NH resulted in scaffolds with improved permeability, while *N*-methylation of the amides that make up the two transannular hydrogen bonds (the Ala2-NH in **8** and Ile5-NH in **9**) significantly reduced both PAMPA and Caco-2 permeability. The retention times of **8** and **9** were dramatically reduced relative to the parent, and the aqueous solubility of **8** was the highest measured in the entire series. These physicochemical effects are consistent with the perturbation of the scaffolds' respective hydrogen bond networks, also evidenced by the presence of multiple conformers in their proton NMR spectra (Supporting Information).

Methylation of the solvent-exposed NH at position 3 in **10** and **11** (Figure 3) resulted in a 5.7-fold increase in Caco-2

DOI: 10.1021/acs.jmedchem.5b00919
J. Med. Chem. 2015, 58, 7409−7418

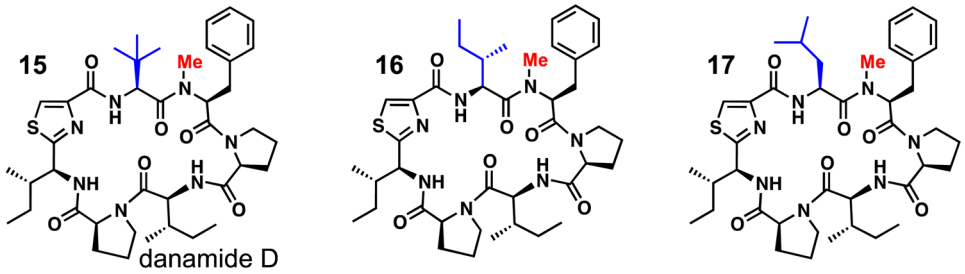

cpd	AlogP	PAMPA P_e (x 10^{-6} cm s^{-1})	Caco-2 P_{app} (x 10^{-6} cm s^{-1})	50% Isocratic RT (min)	Solubility Limit in PBS (μM)	
					Kinetic	Thermodynamic
15	4.20	2.1 ± 1.7	14.0 ± 6.8	10.94	36-44	8 ± 1
16	4.23	1.5 ± 0.2	21.2 ± 2.1	10.00	21-23	12 ± 2
17	4.05	17.2 ± 2.0	19.3 ± 3.3	5.06	133-400	111 ± 38

Figure 5. *N*-Methylated (red) and butyl (blue) side chain analogues of sanguinamide A. **15** Ala2*t*BuGly/Phe(NH) → (NMe), **16** Ala2Ile/Phe(NH) → (NMe), **17** Ala2Leu/Phe(NH) → (NMe). Danamide D, **15**, was previously reported to have impressive cell permeability and oral bioavailability.[30]

permeability relative to the parent and did not disrupt the integrity of the intramolecular hydrogen-bonding network in $CHCl_3$, as shown by T_c-NH data (Table S3, Figure S7). Although only minor retention time differences were observed, **10** and **11** (Figure 3) were significantly more permeable than both the parent compound and all of the *β*-branched analogues discussed previously (Figure 2). Importantly, *N*-methylation at position 3 improved both cell permeability and aqueous solubility.

Side Chain Effects at Position 2. Danamide F (**12**) (Figure 4) has moderate cell permeability (1.2×10^{-6} cm s^{-1}) but remarkable oral bioavailability (F = 51%)[30] compared to that of the parent sanguinamide A (F = 7%).[31] The enhanced oral bioavailability was previously attributed mainly to the steric occlusion of the molecule's polar core by the highly branched, nonproteinogenic *t*BuGly. Since our studies showed that the effects of *β*-branching at the various positions around the ring were relatively minor, we investigated the effect of side chain branching at position 2 in more detail.

Compounds **13** and **14** possess less *β*-branching than **12** at position 2, but retain the same molecular formula (Figure 4). Although the PAMPA permeability of **12** was slightly lower than that of **13** and **14**, all three compounds demonstrated relatively high Caco-2 permeability compared to that of the parent scaffold. No significant difference in Caco-2 permeability was observed across the subseries. Other physicochemical properties including solubility, HPLC retention time (Figure 4), and T_c-NH (Table S3) also varied little across this subseries, consistent with observations by the Fairlie group that the hydrogen bond network is preserved upon substitution of Ala3 with *t*BuGly.[30] Here we show that the use of proteinogenic amino acids is sufficient to impart favorable permeability to this scaffold; whether this effect is due to steric occlusion or simply to the increase in aliphatic character of the side chain relative to Ala cannot be discerned.

***N*-Methylation and *β*-Branched Side Chains at Position 2.** Similar to its non-*N*-methylated analogue danamide F, *N*-methylated danamide D (**15**) (Figure 5) was previously found to have good oral bioavailability (21%) and impressive cell permeability in a low-efflux MDCK (LE-MDCK, also known as RRCK) cell line (9.6×10^{-6} cm s^{-1}).[30] While protein binding may account for the differences in the oral bioavailability of the two danamides, we hypothesized that the differences in passive cell permeability are mainly due to the combined effects of increasing aliphatic character of the side chains and removal of an exposed NH by *N*-methylation.

To investigate the combined effect of side chain *β*-branching and *N*-methylation, we synthesized a subseries based on **15**, which has both a *t*BuGly substitution at position 2 and *N*-methylation at Phe3 (Figure 5). We altered the *β*-branching of the side chain by substituting natural amino acids at position 2, which resulted in slightly better Caco-2 permeabilities for compounds **16** and **17** relative to **15**. In accordance with previous findings,[30] *N*-methylation significantly improved the Caco-2 permeability of all three scaffolds in Figure 5 relative to their non-*N*-methylated counterparts in Figure 4. Together, these data again demonstrate that removal of the solvent-exposed Phe3-NH has a more dramatic effect on permeability than steric shielding by *β*-branching.

Flexibility. Interestingly, **17** is highly permeable in PAMPA while **15** and **16** are not. This divergent behavior is reflected experimentally in the significantly different solubility (Figure 5) and HPLC retention time (Figure S8) of **17**. Although the structural basis for this effect was not immediately obvious, we hypothesized that the PAMPA permeability, HPLC retention time, solubility, and T_c-NH values of compound **17** differed from those of **15** and **16** due to the steric differences imparted by the lack of a *β*-branching methyl in **17**. The *β*-branching could influence polar surface area directly by steric shielding, or by changing the molecule's overall conformation through steric interactions between the side chain and backbone. We set out to test these hypotheses by studying the conformational properties of **15**−**17** in different solvent conditions using a combination of T_c-NH and molecular dynamics (MD) simulations.

In a comparison of T_c-NH in $CDCl_3$ and DMSO (Figure S7),[45] **17** exhibits significantly larger temperature coefficients in DMSO than in $CDCl_3$, suggesting that the polar solvent favors a conformational ensemble with more highly solvent-exposed NH groups, while the nonpolar solvent favors an ensemble in which the NH groups are, on average, more shielded from solvent. Compounds **15** and **16** demonstrate the opposite behavior,

DOI: 10.1021/acs.jmedchem.5b00919
J. Med. Chem. 2015, 58, 7409−7418

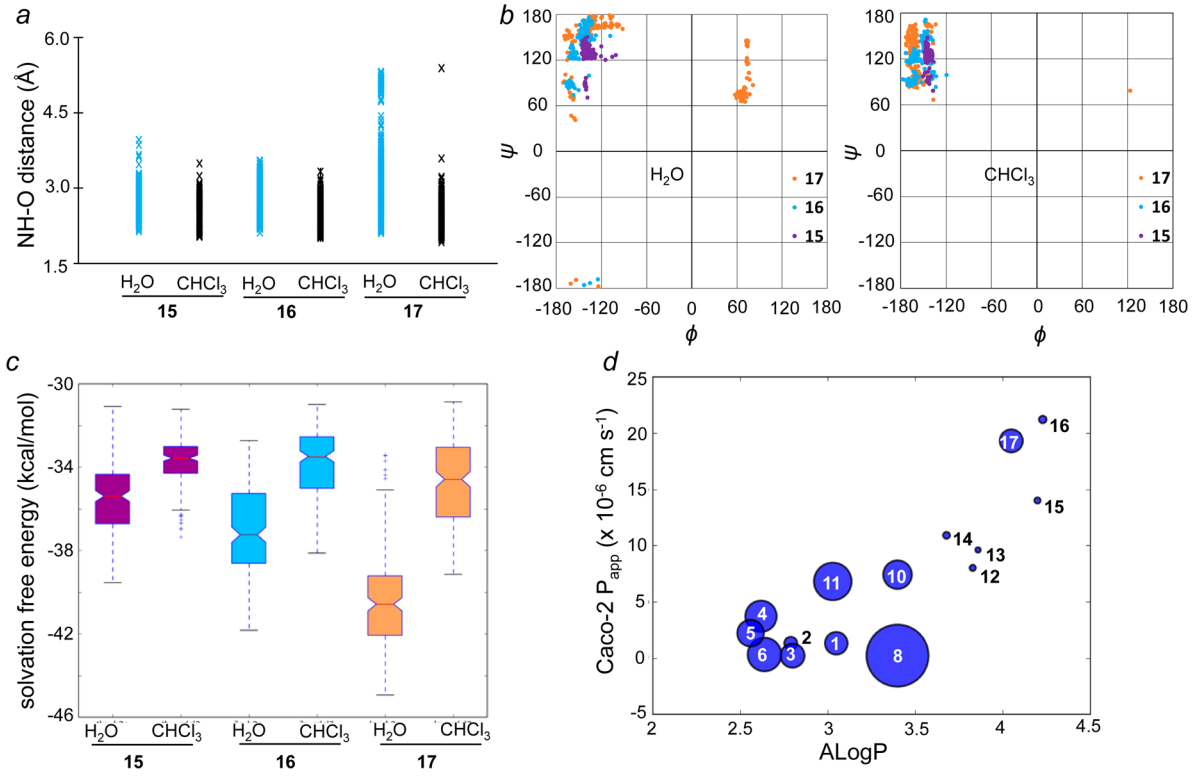

Figure 6. Molecular dynamics simulations in high and low dielectric solvent environments explain physicochemical properties. (a) Hydrogen bond lengths of **15**, **16**, and **17**, (b) Ramachandran plot of ϕ and ψ angles of all conformers of **15** (purple), **16** (blue), and **17** (orange). (c) Solvation free energy in chloroform and water for all MD snapshots of **15** (purple), **16** (blue), and **17** (orange). Red lines designate means. (d) Caco-2 permeability vs AlogP of all macrocycles. Relative thermodynamic solubility correlates to the size of the marker. **17** demonstrates exceptional solubility for its AlogP.

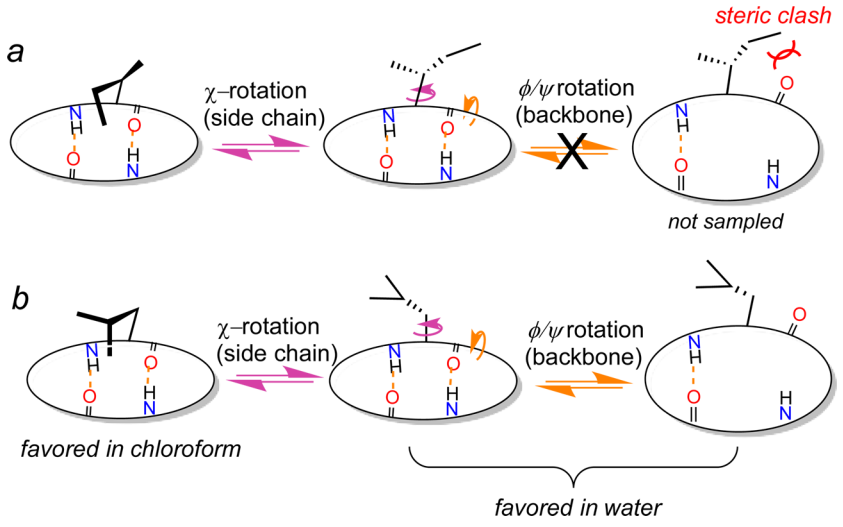

Figure 7. Cell permeability vs aqueous solubility of **16** (top) and **17** (bottom) in low and high dielectric solvent environments. Both the left and middle side chain rotamers are accessible by **16** and **17**, but only **17** is able to adopt the backbone conformer to the right. In the left-most conformer, the Ile and Leu side chains sterically shield the polar core of the macrocycle. In the conformers in the center, χ^1 rotamers expose the polar core. The "open" conformers to the right, only accessed by **17**, have one hydrogen bond and a lower average energy of desolvation in water than any conformer of **15** or **16**. Like **16**, **15** (not shown) cannot sample an "open" conformation due to steric constraints.

where temperature coefficients are smaller in DMSO than those in $CDCl_3$. These data support the hypothesis that **17** has a more dynamic, solvent-dependent,[20,46] structure than the other two macrocycles.

Molecular dynamics simulations were used to further investigate the flexibility of scaffolds **15**–**17** in implicit high- and low-dielectric solvent models. Hydrogen bond lengths, χ^1, ϕ, and ψ angles of residue 2, and solvation energies were monitored in 200 snapshots taken over a 50 ns simulation (Figure 6, Figure S3). While **15** and **16** retained similar H-bond lengths in different dielectric solvent environments (Figure 6a,c), **17** demonstrated significant solvent sensitivity, adopting a single major conformer with short H-bonds in the chloroform simulation while interconverting between at least two different conformer families

DOI: 10.1021/acs.jmedchem.5b00919
J. Med. Chem. 2015, 58, 7409–7418

in the high dielectric simulation. One of the high dielectric conformers was much more open than the other conformers, with only one internal H-bond and the other NH flipped outward toward solvent (Figure 6b,c). In the open conformation of **17**, the Leu residue accessed ϕ and ψ angles (ϕ: 70°, ψ: 70°−150°) known to be highly disfavored for β-branched residues in proteins due to the steric interaction between the side chain and neighboring carbonyl (Figure 6b).[41] Thus, the presence of a β-branched amino acid at position 2 limits scaffold flexibility, while replacement with a Leu residue allows for greater sampling of Ramachandran space. All three compounds had comparable solvation energies in chloroform (Figure 6c), representing their abilities to hide backbone polarity in a low dielectric solvent environment (Figure 7). In contrast, solvation energy in water varied across the series reflecting the dramatically enhanced aqueous solubility of **17** compared to the other two compounds in the series (Figure 6c).

The molecular dynamics data suggest that the relative flexibility of **17** in the high dielectric is permitted by a combination of *N*-methylation and the absence of β-branching. This flexibility affords **17** greater aqueous solubility and a shorter HPLC retention time than **15** and **16** (Figure 6d), while allowing it to maintain very good permeability. In the low dielectric environment of the membrane **17** maintains a rigid, lipophilic conformation with strong intramolecular hydrogen bonds, but in higher dielectric solvents (i.e., isocratic RP-HPLC or aqueous buffer) the scaffold can adopt less lipophilic conformations which allow for an increased solubility and shorter retention time.

DISCUSSION

Although the degree of β-branching correlated slightly with permeability in our side chain variants of sanguinamide A (Figure S4), this modification alone did not have a strong impact on permeability. Other factors, such as overall lipophilicity, solubility, and backbone flexibility were more influential on passive permeability than the effects of steric occlusion imparted by β-branching. Steric shielding of polar groups, and/or structural rigidification imparted by β-branched residues certainly could play a role in driving the permeability of some cyclic peptide natural products, but the effect is not generalizable and did not outweigh the influence of intramolecular hydrogen bonding, *N*-methylation, and aliphatic carbon count in this series.

In several instances, differences were observed between the PAMPA and Caco-2 permeabilities. These differences have been observed previously and may be due to differences in formulation, solubility, and/or plate adhesion. Active uptake mechanisms and efflux pumps may lead to further discrepancies between the two systems. While we suspect that the unique solubility of compound **17** is responsible for its high permeability in both systems, the lack of congruence between the two systems for many of the compounds studied remains an open question.

Substituting the Ala2 side chain in sanguinamide A with *t*BuGly, Ile, or Leu (**12**−**14**) led, on average, to a 9.5-fold increase in Caco-2 cell permeability in this subseries (Figure 4). There was also a significant drop in aqueous solubility, consistent with the ∼0.8 unit increase in AlogP between sanguinamide and its butylated analogues. Within this series, the three analogues had similar cell permeabilities, solubilities, and T_c-NH values (Table S3), suggesting that, consistent with previous observations,[30,31] the Ala2 substitutions maintained the structural rigidity of the parent backbone.

The increase in side chain lipophilicity in **12**−**14** led to a dramatic decrease in thermodynamic aqueous solubility, from 107 μM in sanguinamide A to an average of ∼8 μM for **12**−**14**. In contrast, *N*-methylation at Phe3 surprisingly[26] *increased* solubility compared to sanguinamide A, to 172 μM for compound **10**. Therefore, *N*-methylation of solvent-exposed amides can simultaneously improve both permeability and solubility, possibly by removing a polar NH group that not only impedes permeability, but also decreases solubility by promoting aggregation through intermolecular hydrogen bonding.

Backbone *N*-methylation of the exposed Phe3 amide of sanguinamide A led to a 5.7-fold increase in cell permeability in Caco-2 cells (Figure 3). In contrast, *N*-methylation of the two amides involved in intramolecular hydrogen bonds abrogated permeability. These results highlight the highly specific relationship between *N*-methylation, conformation, and permeability in cyclic peptides, and reinforce the idea that regioselective *N*-methylation is a powerful tool for increasing the passive permeability of cyclic peptides.[6,11,24,26]

Individually, both substitution with larger aliphatic groups at position 2 and *N*-methylation of the solvent-exposed amide at Phe3 led to compounds with improved cell permeability. Combining these substitutions (**15**−**17**) (Figure 5), had an additive effect on Caco-2 permeability, with an average ∼18-fold increase in permeability for the doubly substituted compounds relative to sanguinamide A. This observation is consistent with the findings of Nielsen et al., who reported the *t*BuGly2/(NMe)Phe3 bis-substutited danamide D (**15**) to be 14-fold more cell permeable than sanguinamide A in RRCK cells, and 8-fold more permeable than the singly substituted *t*BuGly2/(NH)Phe3 danamide F (**12**).[30]

The combined effect of *t*BuGly2/(NMe)Phe3 causes significant steric interactions with the backbone, which impart greater flexibility to the molecule and partially expose the polar core.[30] This observation is supported by our own T_c-NH data in $CDCl_3$ (Table S3, Figure S7) showing that *N*-methylation at Phe3 causes an increase in backbone flexibility when position 2 is *t*BuGly or Ile, but not Leu or Ala. Nielsen et al., suggest that this increased flexibility results in greater exposure of polar groups is therefore responsible for the paradoxical decrease in oral bioavailability of the *N*-methylated danamide D (**15**) compared to non-*N*-methylated danamide F (**12**).[30] This hypothesis, however, does not explain the trend in cell permeabilities observed in the same series. Since **12** and **15** have virtually the same aqueous solubility and passive permeability, it is possible that the differences in oral bioavailability and other ADME properties observed previously[30] are due to differences in aliphatic carbon count rather than to a more subtle steric effect on backbone flexibility.

While the aliphatic carbon count remains the major driver of permeability in our series, we also found that flexibility can have a profound and beneficial effect on the properties of these derivatives. In contrast to the difference in flexibility between **12** and **15**[30] caused by a steric interaction between the bulky side chain and *N*-methyl, we found that relieving this steric strain by replacing the *t*BuGly with (**15**) with Leu (**17**) led to an even more pronounced, solvent-dependent conformational flexibility, resulting in a ∼10-fold increase in solubility without any loss in Caco-2 permeability. Our NMR studies show that while **17** is more rigid than its β-branched isomers **15** and **16** in $CDCl_3$, it is more flexible than these isomers in DMSO-d_6. Molecular dynamics studies in high and low dielectric solvent environments corroborate these results and lend insight into the nature of the flexibility differences in this series. This allows **17** to sample open, soluble conformations in water, while adopting a closed,

DOI: 10.1021/acs.jmedchem.5b00919
J. Med. Chem. 2015, 58, 7409−7418

lipophilic conformation in the membrane (Figure 7). Though flexible in water, **17** has the most positive T_c-NH values of all the analogues in $CDCl_3$ (Figure S7 and Table S2), which may represent shorter hydrogen bond distances due to reduced steric repulsion between the β-branched residue at position 2 and the neighboring *N*-methyl.[47] Although the Leu side chain of **17** is not β-branched, we provide computational evidence that it too is capable of sterically shielding the polar core of the macrocycle in a low dielectric solvent environment (Figure 7, Figure S2, and Figure S3), to prevent solvent-exposure of the polar core. The Leu side chain was previously observed shielding the polar core of a cyclic peptide in a different synthetic model system.[16] While the β-branched side chains of **15** and **16** sterically restrict access to "open" conformations in high dielectric solvent environments, the methylene of Leu in **17** permits the backbone flexibility necessary to break intramolecular hydrogen bonds (Figure 7). In a solvent-dependent way, the Leu residue enhances the solubility of the scaffold while maintaining its permeability.

We observe, generally, that the best predictor of Caco-2 permeability in this series was not the degree of β-branching (Figure S4) or HPLC retention time (Figure S5), but rather AlogP (Figure 6d). AlogP calculations do not take 3D structure into account, but the atomistic estimation of lipophilicity works well for this series, in which the majority of compounds have two intramolecular hydrogen bonds and similar backbone geometry. Generally, high Caco-2 permeability was accompanied by low solubility, with the notable exception of compound **17** (Figure 6d). PAMPA permeability correlates well with Caco-2 permeability except for compounds with low aqueous solubility (<100 μM) (Figure S6). We hypothesize that, in addition to preventing aggregation and plate adhesion, solubility could be responsible for the rate of migration out of the lipophilic membrane in PAMPA. It is important to note that the scaffolds in this series become more cell-permeable as their AlogP increases, and that even for the higher AlogP compounds, the permeability continues to increase with increasing lipophilicity (Figure 6d). These findings suggest that, though the MW is approaching 800, the optimal AlogP for the passive cell permeability of this scaffold may be higher than our maximum of 4.23. Beyond this point, however, it becomes more likely that solubility will decrease unless a water-soluble conformer can also be accessed. Lipophilicity and solubility define the limits of a permeability window currently best accessed, in this series, by compound **17**.

By introducing the *t*BuGly residue on the *N*-methylated sanguinamide scaffold (**15**), Nielsen et al. accessed a cell-permeable scaffold, but at the cost of decreased solubility and increased potential for protein binding, which could have negatively impacted oral bioavailability.[30] To balance these factors, we were able to increase lipophilicity of the scaffold while also improving solubility. We found it was best to increase aliphatic carbon count, *N*-methylate exposed H-bond donors, and concurrently limit β-branching to permit greater scaffold flexibility and aqueous solubility.

As for any other drug class, modifications to cyclic peptides designed to improve physical properties such as permeability, and solubility will often result in diminished biological activity. Attempts to improve cell permeability in bioactive cyclic peptides, for example by systematically *N*-methylating backbone amides, have often resulted in significant losses in potency.[25,27,48] This trend is perhaps not surprising given that *N*-methylation may not only remove important polar contacts with the target (and replace them with sterically clashing methyl groups), but may also alter binding by changing the global conformation of the molecule. Furthermore, as seen with compounds **8** and **9**, by abrogating intramolecular hydrogen bonds *N*-methylation may, in some cases, *decrease* permeability. However, we and others have also shown that physical properties in cyclic peptides can also be modulated at the side chain level with changes that have minimal effects on backbone conformation.[16,30] This interplay between the backbone and side chains suggests that the best approach to designing therapeutic cyclic peptides may be to optimize bioactivity and physical properties simultaneously rather than sequentially, as is often the practice.

CONCLUSION

We generated a series of β-branched, *N*-methylated, and side chain-substituted sanguinamide A analogues and assessed each for multiple physicochemical properties to delineate the effects imparted by each structural variable. We determined that in this intramolecularly hydrogen-bonded peptide macrocycle, *N*-methylation and side chain elongation are more effective at improving the passive membrane permeability than is steric occlusion by β-branching. Our findings suggest the β-branching groups can sometimes be involved in steric interactions that increase scaffold rigidity and may have a negative impact on desirable physicochemical properties. The prevalence of β-branched amino acids in cyclic natural products may be driven by evolutionary factors other than permeability, but we cannot fully discount their potential benefits to other scaffolds. A combination of both *N*-methylation and extension of aliphatic side chains produced the scaffolds with the highest cell permeability, with a roughly additive increase in permeability. We also confirmed solubility as a major contributor to the effectiveness of passive membrane permeation.[26] Compound **17**, which demonstrates an unusual combination of excellent passive membrane permeability *and* aqueous solubility, is a promising candidate for the further investigation of high-molecular weight passive membrane permeating cyclic peptides.

EXPERIMENTAL PROCEDURES

General. A detailed description of materials and methods is provided in the Supporting Information.

Peptide Synthesis. Sanguinamide A and its analogues were synthesized using the Fmoc solid-phase synthesis reported by Nielsen,[31] and cyclized in a solution of 1:1 THF/ACN with 3 equiv of HBTU and 6 equiv of DIPEA. Products were analyzed and purified by mass-directed collection with a Waters MicromassZQ mass spec RP-HPLC system. Despite the presence of Pro residues, which are prone to cis/trans isomerization, only one conformer was observed for each macrocycle by HPLC. Cyclic peptide yields ranged from 5% to 30%, with lower yields for the methylated and *tert*-butyl analogues. Cyclic peptides were ≥95% pure by HPLC. The thiazole-containing amino acid monomers were synthesized from enantiomerically pure starting material, as described by Nielsen.[31] *N*-Methylated amino acids were synthesized via the reduction of oxazolidinones described by Freidinger.[49]

PAMPA Studies.[50] A 96-well filter plate with 0.45 μm hydrophobic Immobilon-P membrane supports (Millipore) was loaded with 1% lecithin in dodecane. Samples (10 μM in PBS, pH 7.4) were run for 10 h at 25 °C and pH 7.4, and the concentration of compound in the donor and acceptor wells quantified by LC-MS (Finnigan MAT LTQ using a Phenomonex synergi 2.5 μm, 30 × 2.00 mm Fushion RP10 column with a 0.20 mL/min flow rate) with an internal standard. Samples were run in triplicate and a propranolol standard was included in every plate. See SI for further information.

Caco-2 Studies. Samples (10 μM) were incubated for 2 h at 37 °C with Caco-2 cells in duplicate against atenolol, propranolol, and talinolol standards. LC-MS/MS was used to quantify the concentrations in the

DOI: 10.1021/acs.jmedchem.5b00919
J. Med. Chem. 2015, 58, 7409−7418

apical and basolateral compartments to calculate flux. See SI for further information.

HPLC Retention Time. All compounds were run on 12 min isocratic acetonitrile/water (0.1% formic acid) HPLC gradients on a 3.5 μm C18 (XBridge, 50 mm × 4.6 mm) column at 1.2 mL/min to assess relative lipophilicty.[51]

AlogP. AlogP[52] values were calculated using Virtual Computational Chemistry Laboratory http://wwww.vcclab.org.[53]

Solubility. For kinetic solubility, DMSO stocks of compound (1 μL, 50 mM) were added to 100 μL of PBS (pH 7.4) and sonicated. The solution was incrementally diluted with PBS and sonicated until solid completely dissolved. For thermodynamic solubility, saturated solutions of compounds in PBS were shaken at room temperature for 48 h. The solutions were centrifuged in an Eppendorf 5415 c at 14 000 rpm (15996 g) for 40 min, and the supernatant was collected. Concentrations were determined against a standard curve of the parent compound in DMSO (7.8−1000 μM) via LC-UV on a 40−100 ACN:H_2O gradient at 254 nm. Samples were run in triplicate. See SI for further information.

NMR Experiments. All spectra were recorded on a Varian Inova 600 MHz spectrometer with a 5 mm inverse detection probe at 25 °C, unless otherwise specified. Chemical shifts[47,54] were referenced to $CDCl_3$ at 7.26 ppm or to DMSO-d_6 at 2.50 ppm. Amide temperature coefficient experiments were performed in $CDCl_3$ and DMSO-d_6 at 25°, 30°, 35°, 40°, and 45 °C.

Molecular Dynamics. The NAMD[55] molecular dynamics MD program was used to generate a low energy from arbitrary starting conformers of **15**−**17** that satisfied the NMR restraints reported by Nielsen.[30] Each scaffold underwent a 50 ns simulation at a temperature of 300 K in both chloroform and water represented by a Generalized Born implicit solvent model at dielectric constants of 4 and 80 respectively. Snapshots were acquired every 250 ps, generating an ensemble of 200 conformations for each simulation. The snapshots were minimized before conformational analysis. See SI for further information.

■ ASSOCIATED CONTENT

Supporting Information

The Supporting Information is available free of charge on the ACS Publications website at DOI: 10.1021/acs.jmedchem.5b00919.

Details of PAMPA, and Caco-2 assays, molecular dynamics, NMR spectra, HPLC chromatograms, and temperature coefficient data (PDF)

■ AUTHOR INFORMATION

Corresponding Author

*E-mail: slokey@ucsc.edu; telephone: 831-459-1307.

Author Contributions

A.T.B. and R.S.L. conceived the project. A.T.B. designed all experiments and synthesized all compounds, performed solubility, HPLC, and NMR studies. J.A.S. ran the MD analysis. C.R.P. assisted in developing the MD protocol, calculated solvation energies, and performed database mining. C.E.T. wrote scripts for computational analysis. V.S. assisted in the synthesis of amino acid monomers. M.A.B. managed the acquisition of Caco-2 data. A.T.B., J.A.S., C.R.P., C.E.T, and R.S.L. discussed the results and wrote the paper.

Notes

The authors declare the following competing financial interest(s): R.S.L. is cofounder of Circle Pharma, a macrocycle design company. M.A.B. is an R&D Fellow at Medimmune Ltd.

■ ACKNOWLEDGMENTS

A.T.B. would like to thank Dr. Roger Linington, Dr. Rebecca Braslau, Dr. William Hewitt, Dr. Rushia Turner, Dustin Wride, Dr. Christopher Bailey, and Dr. Kenji Kurita for helpful discussion. This work was supported by funding from Medimmune Ltd.

■ ABBREVIATIONS USED

ADME, absorption distribution metabolism excretion; *t*BuGly, *tert*-butylglycine; PAMPA, parallel artificial membrane permeability assay; THF, tetrahydrofuran; $CHCl_3$, chloroform; $CDCl_3$, deuterated chloroform; HBTU, *N*,*N*,*N*′,*N*′-tetramethyl-*O*-(1*H*-benzotriazol-1-yl)uronium hexafluorophosphate; DIPEA, *N*,*N*-diisopropylethylamine; ACN, acetonitrile; PBS, phosphate-buffered saline; P_{app}, apparent permeability; P_e, effective permeability; RP-HPLC, reverse phase high performance liquid chromatography; RT, retention time; LC/MS, liquid chromatography/mass spectrometry; LC-UV, liquid chromatography ultraviolet; DMSO, dimethyl sulfoxide; Leu, leucine; Ile, isoleucine; Val, valine; Ala, alanine; T_c-NH, amide temperature coefficient

■ REFERENCES

(1) Bhat, A.; Roberts, L. R.; Dwyer, J. J. Lead discovery and optimization strategies for peptide macrocycles. *Eur. J. Med. Chem.* **2015**, *94*, 471−479.

(2) Craik, D. J.; Fairlie, D. P.; Liras, S.; Price, D. The future of peptide-based drugs. *Chem. Biol. Drug Des.* **2013**, *81* (1), 136−147.

(3) Giordanetto, F.; Kihlberg, J. Macrocyclic drugs and clinical candidates: what can medicinal chemists learn from their properties? *J. Med. Chem.* **2014**, *57* (2), 278−295.

(4) Yudin, A. K. Macrocycles: lessons from the distant past, recent developments, and future directions. *Chem. Sci.* **2015**, *6* (1), 30−49.

(5) Burton, P. S.; Conradi, R. A.; Ho, N. F.; Hilgers, A. R.; Borchardt, R. T. How structural features influence the biomembrane permeability of peptides. *J. Pharm. Sci.* **1996**, *85* (12), 1336−1340.

(6) White, T. R.; Renzelman, C. M.; Rand, A. C.; Rezai, T.; McEwen, C. M.; Gelev, V. M.; Turner, R. A.; Linington, R. G.; Leung, S. S.; Kalgutkar, A. S.; Bauman, J. N.; Zhang, Y.; Liras, S.; Price, D. A.; Mathiowetz, A. M.; Jacobson, M. P.; Lokey, R. S. On-resin N-methylation of cyclic peptides for discovery of orally bioavailable scaffolds. *Nat. Chem. Biol.* **2011**, *7* (11), 810−817.

(7) Rezai, T.; Bock, J. E.; Zhou, M. V.; Kalyanaraman, C.; Lokey, R. S.; Jacobson, M. P. Conformational flexibility, internal hydrogen bonding, and passive membrane permeability: successful in silico prediction of the relative permeabilities of cyclic peptides. *J. Am. Chem. Soc.* **2006**, *128* (43), 14073−14080.

(8) Rezai, T.; Yu, B.; Millhauser, G. L.; Jacobson, M. P.; Lokey, R. S. Testing the conformational hypothesis of passive membrane permeability using synthetic cyclic peptide diastereomers. *J. Am. Chem. Soc.* **2006**, *128* (8), 2510−2511.

(9) Zaretsky, S.; Scully, C. C.; Lough, A. J.; Yudin, A. K. Exocyclic control of turn induction in macrocyclic peptide scaffolds. *Chem. - Eur. J.* **2013**, *19* (52), 17668−17672.

(10) Okumu, F. W.; Pauletti, G. M.; Vander Velde, D. G.; Siahaan, T. J.; Borchardt, R. T. Effect of restricted conformational flexibility on the permeation of model hexapeptides across Caco-2 cell monolayers. *Pharm. Res.* **1997**, *14* (2), 169−175.

(11) Lewis, I.; Schaefer, M.; Wagner, T.; Oberer, L.; Sager, E.; Wipfli, P.; Vorherr, T. A detailed investigation on conformation, permeability and PK properties of two related cyclohexapeptides. *Int. J. Pept. Res. Ther.* **2015**, *21* (2), 205−221.

(12) Hill, T. A.; Shepherd, N. E.; Diness, F.; Fairlie, D. P. Constraining cyclic peptides to mimic protein structure motifs. *Angew. Chem., Int. Ed.* **2014**, *53* (48), 13020−13041.

DOI: 10.1021/acs.jmedchem.5b00919
J. Med. Chem. 2015, 58, 7409−7418

(13) Hill, T. A.; Lohman, R. J.; Hoang, H. N.; Nielsen, D. S.; Scully, C. C.; Kok, W. M.; Liu, L.; Lucke, A. J.; Stoermer, M. J.; Schroeder, C. I.; Chaousis, S.; Colless, B.; Bernhardt, P. V.; Edmonds, D. J.; Griffith, D. A.; Rotter, C. J.; Ruggeri, R. B.; Price, D. A.; Liras, S.; Craik, D. J.; Fairlie, D. P. Cyclic penta- and hexaleucine peptides without N-methylation are orally absorbed. *ACS Med. Chem. Lett.* **2014**, *5* (10), 1148−1151.
(14) Beck, J. G.; Chatterjee, J.; Laufer, B.; Kiran, M. U.; Frank, A. O.; Neubauer, S.; Ovadia, O.; Greenberg, S.; Gilon, C.; Hoffman, A.; Kessler, H. Intestinal permeability of cyclic peptides: common key backbone motifs identified. *J. Am. Chem. Soc.* **2012**, *134* (29), 12125−12133.
(15) Bockus, A. T.; McEwen, C. M.; Lokey, R. S. Form and function in cyclic peptide natural products: a pharmacokinetic perspective. *Curr. Top. Med. Chem.* **2013**, *13* (7), 821−836.
(16) Hewitt, W. M.; Leung, S. S.; Pye, C. R.; Ponkey, A. R.; Bednarek, M.; Jacobson, M. P.; Lokey, R. S. Cell-permeable cyclic peptides from synthetic libraries inspired by natural products. *J. Am. Chem. Soc.* **2015**, *137* (2), 715−721.
(17) Schwochert, J.; Pye, C.; Ahlbach, C.; Abdollahian, Y.; Farley, K.; Khunte, B.; Limberakis, C.; Kalgutkar, A. S.; Eng, H.; Shapiro, M. J.; Mathiowetz, A. M.; Price, D. A.; Liras, S.; Lokey, R. S. Revisiting N-to-O acyl shift for synthesis of natural product-like cyclic depsipeptides. *Org. Lett.* **2014**, *16* (23), 6088−6091.
(18) Bock, J. E.; Gavenonis, J.; Kritzer, J. A. Getting in shape: controlling peptide bioactivity and bioavailability using conformational constraints. *ACS Chem. Biol.* **2013**, *8* (3), 488−499.
(19) Yu, H.; Lin, Y. S. Toward structure prediction of cyclic peptides. *Phys. Chem. Chem. Phys.* **2015**, *17* (6), 4210−4219.
(20) Merten, C.; Li, F.; Bravo-Rodriguez, K.; Sanchez-Garcia, E.; Xu, Y.; Sander, W. Solvent-induced conformational changes in cyclic peptides: a vibrational circular dichroism study. *Phys. Chem. Chem. Phys.* **2014**, *16* (12), 5627−5633.
(21) Kessler, H.; Kock, M.; Wein, T.; Gehrke, M. Reinvestigation of the conformation of cyclosporine A in chloroform. *Helv. Chim. Acta* **1990**, *73* (7), 1818−1832.
(22) Ahlbach, C. L.; Lexa, K. W.; Bockus, A. T.; Chen, V.; Crews, P.; Jacobson, M. P.; Lokey, R. S. Beyond cyclosporine A: conformation-dependent passive membrane permeabilities of cyclic peptide natural products. *Future Med. Chem.* **2015**, 1.
(23) Ovadia, O.; Greenberg, S.; Chatterjee, J.; Laufer, B.; Opperer, F.; Kessler, H.; Gilon, C.; Hoffman, A. The effect of multiple N-methylation on intestinal permeability of cyclic hexapeptides. *Mol. Pharmaceutics* **2011**, *8* (2), 479−487.
(24) Wang, C. K.; Northfield, S. E.; Colless, B.; Chaousis, S.; Hamernig, I.; Lohman, R. J.; Nielsen, D. S.; Schroeder, C. I.; Liras, S.; Price, D. A.; Fairlie, D. P.; Craik, D. J. Rational design and synthesis of an orally bioavailable peptide guided by NMR amide temperature coefficients. *Proc. Natl. Acad. Sci. U. S. A.* **2014**, *111* (49), 17504−17509.
(25) Biron, E.; Chatterjee, J.; Ovadia, O.; Langenegger, D.; Brueggen, J.; Hoyer, D.; Schmid, H. A.; Jelinek, R.; Gilon, C.; Hoffman, A.; Kessler, H. Improving oral bioavailability of peptides by multiple N-methylation: somatostatin analogues. *Angew. Chem., Int. Ed.* **2008**, *47* (14), 2595−2599.
(26) Thansandote, P.; Harris, R. M.; Dexter, H. L.; Simpson, G. L.; Pal, S.; Upton, R. J.; Valko, K. Improving the passive permeability of macrocyclic peptides: balancing permeability with other physicochemical properties. *Bioorg. Med. Chem.* **2015**, *23* (2), 322−327.
(27) Chatterjee, J.; Gilon, C.; Hoffman, A.; Kessler, H. N-methylation of peptides: a new perspective in medicinal chemistry. *Acc. Chem. Res.* **2008**, *41* (10), 1331−1342.
(28) Alex, A.; Millan, D. S.; Perez, M.; Wakenhut, F.; Whitlock, G. A. Intramolecular hydrogen bonding to improve membrane permeability and absorption in beyond rule of five chemical space. *MedChemComm* **2011**, *2* (7), 669−674.
(29) Ettorre, A.; D'Andrea, P.; Mauro, S.; Porcelloni, M.; Rossi, C.; Altamura, M.; Catalioto, R. M.; Giuliani, S.; Maggi, C. A.; Fattori, D. hNK2 receptor antagonists. The use of intramolecular hydrogen bonding to increase solubility and membrane permeability. *Bioorg. Med. Chem. Lett.* **2011**, *21* (6), 1807−1809.
(30) Nielsen, D. S.; Hoang, H. N.; Lohman, R. J.; Hill, T. A.; Lucke, A. J.; Craik, D. J.; Edmonds, D. J.; Griffith, D. A.; Rotter, C. J.; Ruggeri, R. B.; Price, D. A.; Liras, S.; Fairlie, D. P. Improving on nature: making a cyclic heptapeptide orally bioavailable. *Angew. Chem., Int. Ed.* **2014**, *53* (45), 12059−12063.
(31) Nielsen, D. S.; Hoang, H. N.; Lohman, R. J.; Diness, F.; Fairlie, D. P. Total synthesis, structure, and oral absorption of a thiazole cyclic peptide, sanguinamide A. *Org. Lett.* **2012**, *14* (22), 5720−5723.
(32) Lipinski, C. A.; Lombardo, F.; Dominy, B. W.; Feeney, P. J. Experimental and computational approaches to estimate solubility and permeability in drug discovery and development settings. *Adv. Drug Delivery Rev.* **1997**, *23* (1−3), 3−25.
(33) Camenisch, G.; Alsenz, J.; van de Waterbeemd, H.; Folkers, G. Estimation of permeability by passive diffusion through Caco-2 cell monolayers using the drugs' lipophilicity and molecular weight. *Eur. J. Pharm. Sci.* **1998**, *6* (4), 313−319.
(34) Doak, B. C.; Over, B.; Giordanetto, F.; Kihlberg, J. Oral druggable space beyond the rule of 5: insights from drugs and clinical candidates. *Chem. Biol.* **2014**, *21* (9), 1115−1142.
(35) Goetz, G. H.; Philippe, L.; Shapiro, M. J. EPSA: a novel supercritical fluid chromatography technique enabling the design of permeable cyclic peptides. *ACS Med. Chem. Lett.* **2014**, *5* (10), 1167−1172.
(36) Di, L. Strategic approaches to optimizing peptide ADME properties. *AAPS J.* **2015**, *17* (1), 134−143.
(37) Wang, C. K.; Northfield, S. E.; Swedberg, J. E.; Colless, B.; Chaousis, S.; Price, D. A.; Liras, S.; Craik, D. J. Exploring experimental and computational markers of cyclic peptides: charting islands of permeability. *Eur. J. Med. Chem.* **2015**, *97*, 202−213.
(38) Rand, A. C.; Leung, S. S. F.; Eng, H.; Rotter, C. J.; Sharma, R.; Kalgutkar, A. S.; Zhang, Y. Z.; Varma, M. V.; Farley, K. A.; Khunte, B.; Limberakis, C.; Price, D. A.; Liras, S.; Mathiowetz, A. M.; Jacobson, M. P.; Lokey, R. S. Optimizing PK properties of cyclic peptides: the effect of side chain substitutions on permeability and clearance. *MedChemComm* **2012**, *3* (10), 1282−1289.
(39) Schwochert, J.; Turner, R.; Thang, M.; Berkeley, R. F.; Ponkey, A. R.; Rodriguez, K. M.; Leung, S. S.; Khunte, B.; Goetz, G.; Limberakis, C.; Kalgutkar, A. S.; Eng, H.; Shapiro, M. J.; Mathiowetz, A. M.; Price, D. A.; Liras, S.; Jacobson, M. P.; Lokey, R. S. Peptide to peptoid substitutions increase cell permeability in cyclic hexapeptides. *Org. Lett.* **2015**, *17* (12), 2928−2931.
(40) Bockus, A. T.; Lexa, K. W.; Pye, C. R.; Kalgutkar, A. S.; Gardner, J. W.; Hund, K. C.; Hewitt, W. M.; Schwochert, J. A.; Glassey, E.; Price, D. A.; Mathiowetz, A. M.; Liras, S.; Jacobson, M. P.; Lokey, R. S. Probing the physicochemical boundaries of cell permeability and oral bioavailability in lipophilic macrocycles inspired by natural products. *J. Med. Chem.* **2015**, *58* (11), 4581−4589.
(41) Zhou, A. Q.; Caballero, D.; O'Hern, C. S.; Regan, L. New insights into the interdependence between amino acid stereochemistry and protein structure. *Biophys. J.* **2013**, *105* (10), 2403−2411.
(42) Dalisay, D. S.; Rogers, E. W.; Edison, A. S.; Molinski, T. F. Structure elucidation at the nanomole scale. 1. Trisoxazole macrolides and thiazole-containing cyclic peptides from the nudibranch Hexabranchus sanguineus. *J. Nat. Prod.* **2009**, *72* (4), 732−738.
(43) Gasteiger, E., Hoogland, C., Gattiker, A., Duvaud, S., Wilkins, M. R., Appel, R. D., Bairoch, A., Protein identification and analysis tools on the ExPASy server. In *The Proteomics Protocols Handbook*; Walker, J. M., Ed.; Humana Press: New York, 2005; pp 571−607.
(44) Houssen, W. E.; Jaspars, M. Azole-based cyclic peptides from the sea squirt Lissoclinum patella: old scaffolds, new avenues. *ChemBioChem* **2010**, *11* (13), 1803−1815.
(45) Abraham, M. H.; Abraham, R. J.; Acree, W. E., Jr.; Aliev, A. E.; Leo, A. J.; Whaley, W. L. An NMR method for the quantitative assessment of intramolecular hydrogen bonding; application to physicochemical, environmental, and biochemical properties. *J. Org. Chem.* **2014**, *79* (22), 11075−11083.
(46) Milne, B. F.; Morris, L. A.; Jaspars, M.; Thompson, G. S. Conformational change in the thiazole and oxazoline containing cyclic

DOI: 10.1021/acs.jmedchem.5b00919
J. Med. Chem. 2015, 58, 7409−7418

octapeptides, the patellamides. Part 2. Solvent dependent conformational change. *J. Chem. Soc., Perkin Trans. 2* **2002**, No. 6, 1076−1080.
(47) Hong, J.; Jing, Q.; Yao, L. The protein amide (1)H(N) chemical shift temperature coefficient reflects thermal expansion of the N-H···O═C hydrogen bond. *J. Biomol. NMR* **2013**, *55* (1), 71−78.
(48) Doedens, L.; Opperer, F.; Cai, M.; Beck, J. G.; Dedek, M.; Palmer, E.; Hruby, V. J.; Kessler, H. Multiple N-methylation of MT-II backbone amide bonds leads to melanocortin receptor subtype hMC1R selectivity: pharmacological and conformational studies. *J. Am. Chem. Soc.* **2010**, *132* (23), 8115−8128.
(49) Freidinger, R. M.; Hinkle, J. S.; Perlow, D. S.; Arison, B. H. Synthesis of 9-fluorenylmethyloxycarbonyl-protected N-alkyl amino-acids by reduction of oxazolidinones. *J. Org. Chem.* **1983**, *48* (1), 77−81.
(50) Kansy, M.; Senner, F.; Gubernator, K. Physicochemical high throughput screening: parallel artificial membrane permeation assay in the description of passive absorption processes. *J. Med. Chem.* **1998**, *41* (7), 1007−1010.
(51) Valko, K., Application of high performance liquid chromatography for the measurements of lipophilicity and bio-mimetic binding properties in drug discovery. In *Physico Chemical Methods in Drug Discovery and Development*; Mandic, Z., Ed.; IAPC Publishing: Zagreb, Croatia, 2012; pp 70−72.
(52) Ghose, A. K.; Viswanadhan, V. N.; Wendoloski, J. J. Prediction of hydrophobic (lipophilic) properties of small organic molecules using fragmental methods: An analysis of ALOGP and CLOGP methods. *J. Phys. Chem. A* **1998**, *102* (21), 3762−3772.
(53) Tetko, I. V.; Gasteiger, J.; Todeschini, R.; Mauri, A.; Livingstone, D.; Ertl, P.; Palyulin, V. A.; Radchenko, E. V.; Zefirov, N. S.; Makarenko, A. S.; Tanchuk, V. Y.; Prokopenko, V. V. Virtual computational chemistry laboratory–design and description. *J. Comput.-Aided Mol. Des.* **2005**, *19* (6), 453−463.
(54) Cierpicki, T.; Otlewski, J. Amide proton temperature coefficients as hydrogen bond indicators in proteins. *J. Biomol. NMR* **2001**, *21* (3), 249−261.
(55) Phillips, J. C.; Braun, R.; Wang, W.; Gumbart, J.; Tajkhorshid, E.; Villa, E.; Chipot, C.; Skeel, R. D.; Kale, L.; Schulten, K. Scalable molecular dynamics with NAMD. *J. Comput. Chem.* **2005**, *26* (16), 1781−1802.

DOI: 10.1021/acs.jmedchem.5b00919
J. Med. Chem. 2015, 58, 7409−7418